

A New UWB-Principle for Sensor-Array Application

J. Sachs¹, P. Peyrerl², M. Roßberg¹

¹Technical University of Ilmenau: e-mail: sac@e-technik.tu-ilmenau.de

²MEODAT GmbH: e-mail: pey@meodat.de

Abstract

The paper presents a simple principle to measure the transfer function or rather the impulse response of ultra-wideband systems. The main aspects of the new measurement head are its flexibility of application, its measurement speed and the possibility of a full circuit integration, which results in small, robust, lightweight and low cost devices with low power consumption. Beside this, the method allows the measurement of multi-port devices and it has a good suppression of perturbation signals. These advantages may be exploited in a great variety of microwave sensing applications, covering single sensor and array arrangements.

1. Introduction

Microwave sensing and imaging in many industrial, medical, geological, environmental and archaeological applications as well as for non-destructive testing in civil engineering or traffic control exploits ultra wideband (UWB) principles. The measurement methods are based on the determination of the frequency or the transient behaviour of a single- or multi-sensor arrangement. As long as the systems under test (SUT) can be considered as linear and time-invariant, the transfer function or impulse response describes them completely. In case of a slow time variation, a SUT may be considered as 'segment-wise' stationary if the repetition rate of the measurement is sufficiently high.

The measurement front-end (sensor electronics), described in the following, is a new principle to determine the impulse response and thus the transfer function for wideband systems. Its main parts serve to generate a wideband stimulus, to capture the SUT response and to calculate the impulse response by an effective correlation algorithm. The electronics are based chiefly on digital circuits which permit good technical and economical parameters by its integration capabilities. The bandwidth B , the (equivalent) observation time T_{eq} , the repetition rate r of the measurement and the dynamic range L_a are the main parameters of the front-end. The bandwidth deter-

mines the range resolution in radar applications. But for radiation in materials (surface penetrating radar - SPR, medical microwave imaging, ...) the operating frequencies should be as low as possible. This often leads to the requirement of a relative bandwidth near 1.

Further features relate to the multi-channel capability of the front-ends. Imaging devices mostly use sensor-arrays, requiring multi-channel high-speed acquisition systems.

Known UWB principles are the classical impulse method (commercialised in most SPR devices), the stepped frequency method, the FMCW method and the noise radar. All of them are not able to meet the requirements of a high resolution, short range, high speed sensing device.

In the following the basic principle for single and multisensor applications will be explained. Further some results received from a test sample in PCB technology will be shown and finally the integration in SiGe technology will be considered.

2. Basic principle

From the viewpoint of linear system theory, some constraints to the measurement system may be introduced. The use of a correlation principle either in the time or frequency domain allows the application of stimulus signals with arbitrary time shape. The only constraint is the spectrum, which should be wide enough. Additionally, low crest factor signals should be preferred in practice due to the limited dynamics of real systems. Further, the use of periodic signals avoids bias errors, allows linear averaging for noise suppression and the signal acquisition may be carried out by undersampling. Thus signals of an extreme bandwidth may be sampled using low cost, commercial ADCs in combination with sampling gates. Finally the generation of the stimulus signal, the correlation and the control of the sampling gate should be as simple as possible.

With the maximum length binary sequence (MLBS), one can meet such requirements. Figure 1 shows its idealised time shape, auto correlation function and spectrum.

An MLBS of order n may be generated by an n -stage shift register using an appropriate feedback. Depending on the circuit technology, its maximum clock rate may be attain 20 GHz and more.

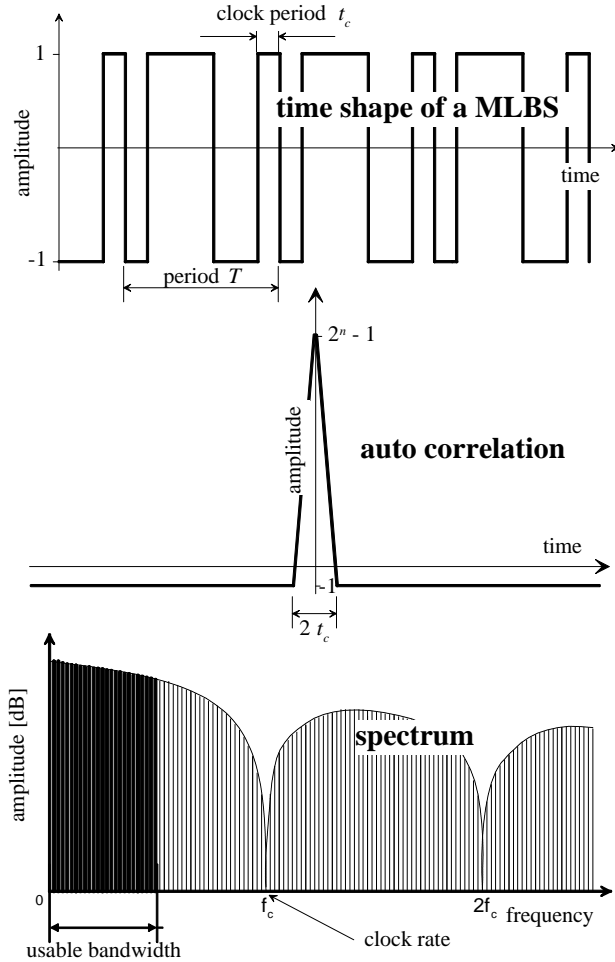


Fig. 1: Time shape, auto correlation function and spectrum of a MLBS. For a better graphical representation the shown spectrum applies to a MLBS of higher order than used in the first and second diagram.

The MLBS period is $T = (2^n - 1)t_c$, where t_c is the period of the system clock. The time T corresponds to the equivalent observation window length $T_{eq} = T$ and should be equal or larger than the observable length of the impulse response of the SUT. Thus the time window T limits the ambiguity range in radar applications or the observable reverberation time of resonant systems.

Regarding the spectrum in figure 1, it is useful to fix the equivalent sampling frequency to the clock frequency $f_c = 1/t_c$, that means one sample per elementary pulse.

Thus the examination bandwidth B is limited to the range $0 \leq f < f_c/2$ of the MLBS-spectrum. To avoid aliasing, either an anti-aliasing filter must be used or the SUT limits the upper frequency band by itself.

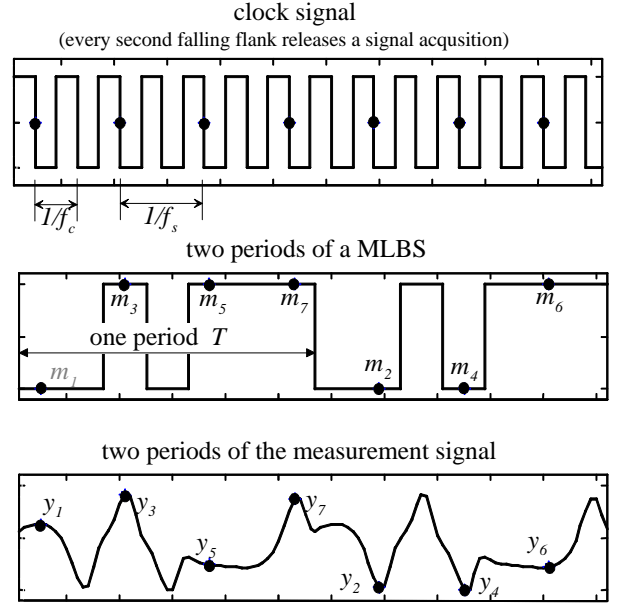


Fig. 2: Acquisition of MLBS-data by interleaved sampling. In this example the sampling clock is the output of a one stage divider, that has the half of the clock rate. The natural order of the signal samples is denoted for both the stimulus and the measurement signal.

The sampling frequency f_s may be simply derived from the clock rate f_c by an m -stage binary clock divider, so that $f_s = 2^{-m} f_c$. Since the period length T of an MLBS always differs by one clock period from a power of two, 2^m periods of the MLBS are needed to acquire the complete data set with the equivalent sampling frequency f_c – one sample per elementary pulse (see figure 2).

The practical implementation of this principle is demonstrated in the block diagram of figure 3. Except for the emphasised part, all components are low cost commercial ICs. The whole system is triggered by the clock generator that pushes an n -stage shift register and an m -stage binary divider. The shift register generates the MLBS stimulus $m(t)$ and the divider delivers the sampling clock f_s , which drives the S&H circuit, the ADC and an averager. Finally, a digital signal processor (DSP) calculates the cross correlation $\mathbf{y}(k)$ which is approximately equal to the impulse response of the system under test $h(k) \cong \mathbf{y}(k)$. From the sampled data $y(l)$, the cross-correlation $\mathbf{y}(k)$ may be determined by the matrix equation (1), which the DSP

solves very quickly using the Hadamard-algorithm [1]. It has a butterfly structure comparable to the FFT algorithm.

$$\begin{bmatrix} \mathbf{Y}_1 \\ \vdots \\ \mathbf{Y}_7 \end{bmatrix} = [y_1 \dots y_7] \begin{bmatrix} m_1 & m_7 & m_6 & \dots & m_2 \\ m_2 & m_1 & m_7 & \dots & m_3 \\ m_3 & m_2 & m_1 & \dots & m_4 \\ m_4 & m_3 & m_2 & \dots & m_5 \\ m_5 & m_4 & m_3 & \dots & m_6 \\ m_6 & m_5 & m_4 & \dots & m_7 \\ m_7 & m_6 & m_5 & \dots & m_1 \end{bmatrix}, m_k \in -1, 1 \quad (1)$$

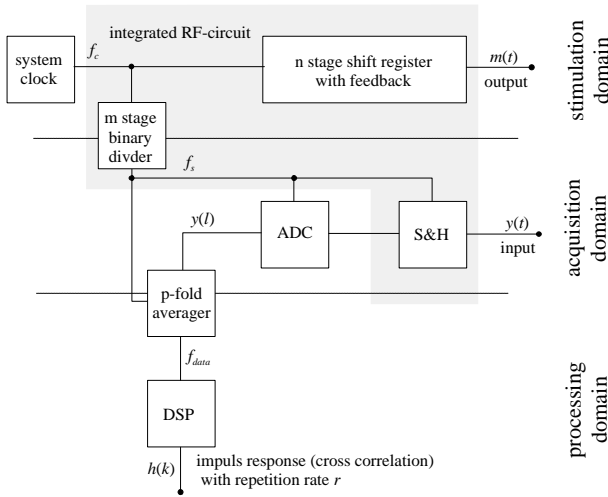


Fig. 3: Block diagram of the UWB front end. The emphasised section should be integrated to achieve a bandwidth greater than 500 MHz.

The p-fold averager matches the signal acquisition rate f_s to the processing speed of the DSP by reducing the data rate to $f_{data} = f_s/p$. Simultaneously it increases the dynamic range of the captured signals. The dynamic range L_a and the overall observation (correlation) time T_{obs} of the UWB-front-end result in:

$$L_a [\text{dB}] \cong 6b + 10 \cdot \lg(p) 2^n - 1 \quad (2)$$

and

$$T_{obs} = \lfloor 2^n - 1 \rfloor 2^m p t_c = \frac{1}{r} < \frac{c}{2 v B}. \quad (3)$$

Here b is the number of effective bits of the acquisition circuitry (S&H and ADC). The suppression (in dB) of noise and other uncorrelated perturbations is given by $10 \cdot \lg_{10}(p(2^n - 1))$. Since the data acquisition works continuously, the measurement rate r is inverse to the time

interval T_{obs} . All samples captured in this time interval lead to one cross correlation $\mathbf{y}(k)$ or impulse response $h(k)$ respectively. In case of moving objects (time variant system), an upper limit of the observation time T_{obs} exists, depending on the propagation velocity c and bandwidth B of the sounding waves as well as the dislocation speed v of the object. Further note the difference between T_{obs} and T_{eq} . Whereas T_{obs} covers the real observation interval, T_{eq} applies to the time scale of the physical process within the SUT omitting undersampling and averaging.

Regarding the block diagram in figure 3 one can divide the UWB front end into three groups of subsystems depending on their processing speed.

1. The stimulation domain has to keep the real time requirements of the physical SUT, i.e. the bandwidth B (clock rate f_c) and period T (number n of stages) of the stimulus. Since all components of the RF circuit are decoupled, it works at any frequency lower than the maximum clock rate. The upper limit of B is imposed by the RF circuit design and may reach 20 GHz and more with sophisticated GaAs technology.

2. The processing speed in the acquisition domain corresponds to the sampling frequency f_s that can be fixed largely independent from f_c by the stage number m of the binary divider. Using an adequate ADC, f_s typically lies in the video range.

3. A similar situation arises with the observation rate r within the processing domain, which is largely decoupled from the acquisition speed by the averaging number p . Generally the observation rate r is limited by the data processing capability of the DSP. A rough estimation for a TMS 320C62 comes to 20.000 observations (impulse responses) per second for an MLBS of order $n = 9$ for example.

This three part structure includes a large degree of freedom to optimise the front end with respect to physical and/or economical demands. If several identical UWB front ends work at a slightly different clock rate f_c (a random hopping of f_c is also possible), they are mutually uncorrelated (supposing a sufficiently long observation time T_{obs}). Therefore different sensors do not interact – an important aspect for the distance measurement of cars and similar applications.

3. Multi-channel application

The investigation of a multi port SUT, i.e. a sensor-array, requires a well synchronised multi-channel measurement system. Figure 4 shows a corresponding arrangement. For this purpose, the RF-ICs have to extend by a clock regeneration circuit to enable a cascaded synchronisation. Further more by means of the procedure control it should be possible to switch the MLBS-signal

$m(t)$ on/off ($A_l = 1$ or 0) or to invert it respectively ($A_l = -1$). Thus the output signal $u_l(t)$ of the l^{th} RF circuit may be written as:

$$u_l(t) \in \{m(t), 0, -m(t)\}$$

$$\Rightarrow u_l(t) = A_l m(t) \quad A_l = -1, 0, 1$$

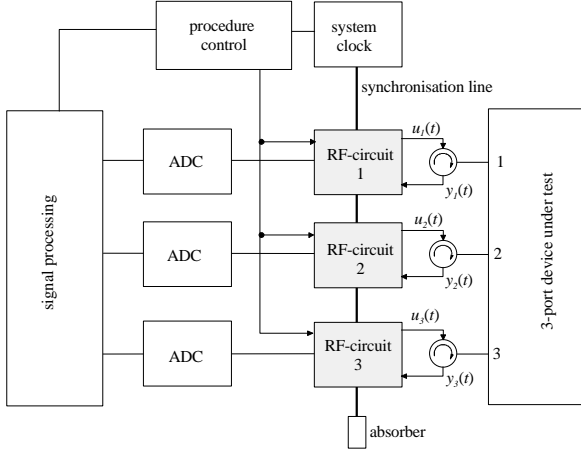


Fig. 4: Simplified block diagram for the multi channel mode

Consider a linear L -port. It is characterised by a set of L^2 impulse responses which may be arranged in the matrix $\mathbf{h}(t)$. The same is true for the matrix $\mathbf{H}(f)$ of the transfer functions. To determine all components of those matrices the complete set of L -channel measurements has to be repeated R times with a set of linear independent stimulus signals. This may be achieved by a proper control of the test signal $u_l(t)$ of the individual channels. The total number of measurements R must be equal or greater than the number of ports L .

In the following, continuous time signals will be considered. The test signals $u_l(t)$ and the receiving signals $y_l(t)$ of all channels and all repetitions of the measurement are ordered in matrices. The number of rows corresponds to the port number L and the column number corresponds to the number of the measurements R .

$$\mathbf{y}(t) = \begin{pmatrix} y_{11}(t) & \cdots & y_{1R}(t) \\ \vdots & \ddots & \vdots \\ y_{L1}(t) & \cdots & y_{LR}(t) \end{pmatrix};$$

$$\mathbf{u}(t) = \begin{pmatrix} u_{11}(t) & \cdots & u_{1R}(t) \\ \vdots & \ddots & \vdots \\ u_{L1}(t) & \cdots & u_{LR}(t) \end{pmatrix} = m(t) \mathbf{A}, \quad A_{ij} = -1, 0, 1$$

The matrix \mathbf{u} of the stimuli may be expressed by the scalar MLBS signal $m(t)$ and the matrix \mathbf{A} representing the state of the procedure control during the individual measurements.

All cross-correlation functions between the input and output signals of the SUT may be written as:

$$\boldsymbol{\psi}(t) = \int \mathbf{y}(t) \mathbf{u}^T dt + t \uparrow dt \quad (4)$$

The matrix $\boldsymbol{\psi}$ of all cross correlation functions is given by:

$$\boldsymbol{\psi}(t) = \begin{pmatrix} y_{11}(t) & \cdots & y_{1L}(t) \\ \vdots & \ddots & \vdots \\ y_{L1}(t) & \cdots & y_{LL}(t) \end{pmatrix}$$

Due to the correlation behaviour of the MLBS, equation (4) may be simplified to

$$\boldsymbol{\psi}(t) \cong \mathbf{h}(t) \mathbf{A} \mathbf{A}^T$$

$$\sim \mathbf{h}(t) \quad \text{if } \mathbf{A} \text{ is orthogonal,} \quad (5)$$

which gives the desired form to determine the complete set of impulse responses.

In a simple case \mathbf{A} could be a diagonal matrix. This means, that, in an alternating manner, always one RF-channel stimulates the SUT while all the others capture the transmitted signals. If the magnitudes of all transfer functions $H_{ij}(f)$ of the SUT are of the same order, the switch matrix \mathbf{A} may also be of Hadamard-type (if a Hadamard-matrix exists for the actual number of ports). Note, that the observation rate r decreases by the number of measurements R .

4. Experimental circuit

For testing the new UWB principle, an experimental circuit was made corresponding to the block scheme of figure 3. Standard PCB technology was used to manufacture all subsystems. Digital high speed components (shift register, binary divider) are based on ECLinPSLite ICs. Figure 5 shows a PCB containing the clock generation, the MLBS shift register (9 stages) and the binary divider. The system clock is delivered by a PLL stabilised VCO. The implemented shift register works with a clock rate up to 1 GHz. With this, the usable bandwidth covers 0 ... 400 MHz approximately (if the whole measurement channel is dc-coupled). The impulse response includes 511 points.

The signal acquisition includes a 500 ps sampler and a 12-bit video ADC followed by a 128-fold averaging. It is carried out by a fast adder modified for this purpose. The correlation and further processing is made by an TMS320C31 board, allowing the calculation of up to

1.000 impulse responses per second (corresponding to a data rate of more than 1 Mbyte/s). Additional processing and data viewing is done on a PC, but with lower data rates. No effort was made to speed up the data transfer, since the actual investigations do not require the full speed. Figure 6 shows the user interface of the UWB designer tool. Its purpose is to investigate UWB parameters related to changes in hard- and software.

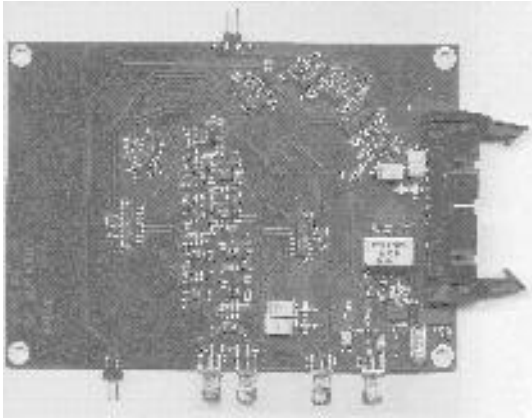


Fig. 5: Photo of the PCB including the RF subsystems - MLBS generator with clock distribution, binary divider and clock generator.

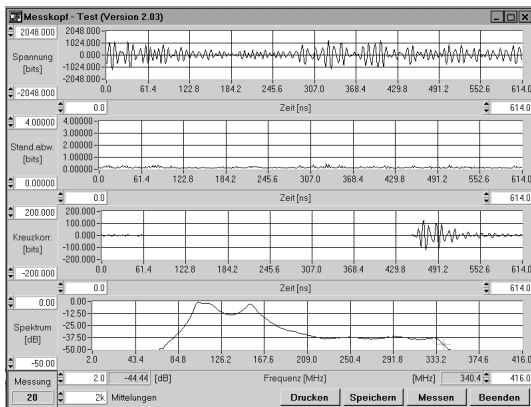


Fig. 6: Hardcopy of the designer tool for the UWB-front-end. The plots are ordered in the following manner:

1. captured time signal
2. standard deviation of time signal
3. impulse response (cross correlation)
4. transfer function (cross spectrum)

In figure 7, the transfer function of a bandpass DUT is shown, measured by both the UWB-head and a network analyser. The differences may be explained due to the fact that for the UWB head only a response calibration was

made. Source match, load match etc. were neglected for simplicity.

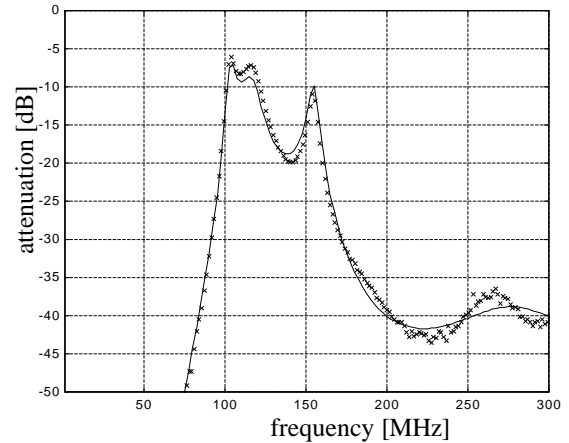


Fig. 7: Magnitude of a transfer function, measured by a network analyser (solid line) and the UWB front end (x-mark). The comparison shows respectable agreements, considering the simple correction of systematic errors.

5. Integrated MLBS Generator

A monolithic integrated circuit generating the MLBS as well as the synchronisation signals for the S&H circuit was designed to overcome the speed limits of a discrete ECL MLBS generator. The IC will be fabricated in Silicon/Silicon-Germanium Heterostructure Bipolar Transistor (Si/SiGe HBT) technology. The Si/SiGe HBT technology is less expensive and provides better heat dissipation compared to III/V compound semiconductor based techniques commonly used for RF applications.

Typical parameters of recently integrated Si/SiGe HBTs are transit frequencies (f_t) and maximum frequencies of oscillation (f_{max}) up to 50 GHz with dc current gains (h_{fe}) over 100. The delay of an ECL or CML gate was found to be in the 20 ... 30 ps-range [2] for the HBT technology the RF chip is designed for.

The generator circuit consists of the following main components:

- a 9-staged feedback shift register to generate the MLBS;
- a synchronised clock divider with controllable divider factors from 2^7 ... 2^{10} for S&H clock generation;
- a low power dissipating internal clock driver capable of driving all internal logic gates;
- a clock input stage providing a 50Ω on chip termination with an input for internal clock enabling;

- differential output drivers for the system clock (may be used for cascading) and the S&H clock.

The circuit was designed in differential ECL. Differential operation is favourable with respect to crosstalk and instability problems as well as low time jitter. The internal voltage swing is 400 mV differential. The external RF output voltage swing is 800 mV into a 100 Ω load for differential operation. All control inputs and outputs are TTL compatible. The operating voltage of the circuit is 5 V from a single power supply. The simulated power consumption of the entire circuit does not exceed 2 Watts.

Figure 8 shows a simulated time segment of the MLBS generated by the circuit. Since all circuit elements are dc coupled, no lower clock frequency limit exists. The simulation leads to clock rates higher than 12 GHz. The rise and fall times of the simulated RF output signals are lower than 30 ps. This promises a bandwidth from 0 up to 5 or 6 GHz.

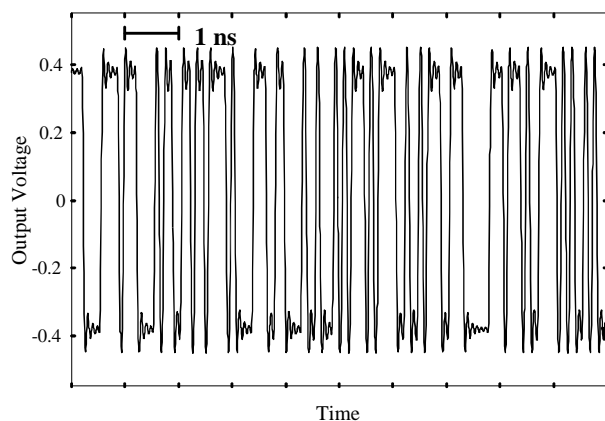


Fig. 8: Simulated output signal of the RF-IC. The shown time window covers approximately the fourth part of the complete period of the stimulus signal at a clock rate of 12 GHz.

6. Summary

The main parts of the UWB front end are based on digital circuits. This causes its flexibility with respect to economical demands and to physical aspects of the objects under test. It seems possible to integrate the front end completely for a certain application on a large scale. On the other hand, integrating only the RF part is sufficient for the most applications. This also allows for a high design flexibility in the front end, because the shift registers and the binary divider can be selected as required. Some features of the shown UWB-principle are summarised below:

- The bandwidth can be adapted simply by adjusting the clock rate f_c .
- In the base band version, the usable spectrum of the stimulus theoretically ranges from dc to half of the clock rate. By adding a carrier and slightly modifying the processing the bandwidth may be extended up to $1,5 f_c$ (not shown in this paper). In the simplest way the clock can be used as the carrier.
- Stimulation rate f_c , acquisition rate f_s and observation rate r are largely decoupled due to the use of interleaved sampling and averaging.
- The observation rate is not limited by transition events within the UWB front end.
- The RF circuit may work either in a high speed or low-speed digital surrounding, so that economical and sweep rate/resolution aspects can be optimised mutually.
- The dynamic range L_d may be increased with a reduction of the observation rate r and vice versa by varying the averaging factor p .
- In contrast to sequential sampling, the interleaved sampling allows the acquisition of more than one sample per period of the stimulus. Thus, the efficiency of exploitation of information in the receiving signals can be chosen in a wide area by the ADC-speed.
- A multi-channel measurement system can be build up by cascading several RF circuits. The complete L-port parameters may be determined by L measurement cycles with appropriate controlled outputs.
- Low electromagnetic interference exists due to the use of spread spectrum signals and the proper choice of the clock rate.
- The RF-generator works in a pure periodic manner. Thus its cross coupling to the receiver (S&H) is of a systematic, periodic nature. In terms of network analyser nomenclature this error correspond to the directivity or isolation error. It may be eliminated by calibration.

References

- [1] N. Xiang: A Mobil Universal Measuring System for the Binaural Room-Acoustic Modelling-Technique. Schriftenreihe der Bundesanstalt für Arbeitsschutz, Fb 611. Dortmund 1991, ISBN 3-89429-028-5
- [2] W. Pierschel, W. Winkler and M. Roßberg: "RF Circuits Fabricated with CMOS-Compatible SiGe HBT Process Module", Proc. of the 5th IEEE ICECS, pp. 179-182, Lisboa 7.-10. Sept. 1998